International Journal of Science Engineering and Advance Technology

A Numerical Model To Predict The Performance Of A CI Engine Enriched By Hydrogen Fuel And Flow Visualization In The Intake Manifold For Hydrogen Injection Using CFD

[1]G.Bala Krishna Reddy , [2]Sammala.Rajasekhar , [3]A.Venkata Sridhar , [4]Y.Dhana Sekhar
[1] M. Tech. Student, [2]Associate.Professor, [3]Associate.Professor,
Dept of ME, KITS, Divili.
[4]Research Scholar

***Abstract*:**

The rapid depletion of fossil fuels has called for the use of alternative fuels in the field of IC engines and combustion. Therefore it is high time to switch over to new design of automobiles with lesser emissions run by alternative gaseous fuels like LPG, CNG, and Hydrogen etc. From the literature survey it is observed that extensive research has been carried out on thermodynamic modeling of diesel engine. The present investigation includes two stages. One is numerical modeling of diesel engine enriched by hydrogen fuel and later, using CFD analysis, the investigation carried on so as to predicting the position of hydrogen gas injector and injection angle for manifold injection of dual fuel diesel engine.

In the first stage, thermodynamic analysis was done using double weibe heat release equation during the combustion period. A MATLAB code has been written for the thermodynamic model, which takes input as engine parameters, fuel data and gives the Pressure-Crank angle, Temperature-Crank angle and Rate of heat release-Crank angle plots. These plots were used to analyze the performance of engine. Further study has been done on effect of intake air temperature on ignition delay period, when the diesel engine enriched by hydrogen gas fuel.

Two cases were considered in the present model, one with diesel as fuel and other with diesel as primary fuel and hydrogen as secondary fuel on mass basis. The peak cylinder pressure of hydrogen enriched CI engine and diesel operated engine are found to be 91.7 bar and 87.1 bar at 1500 rpm respectively. The cylinder temperature of hydrogen enriched CI engine is found to be 1997 K and for diesel operated engine, it was found to be 1898 K at 1500 rpm. The rate of heat release of hydrogen enriched CI engine is found to be 88.2 J/ deg, compared with 86.9 J/ deg for the diesel engine at 1500 rpm. The maximum heat release occurs at nearer to the TDC for hydrogen enriched engine, which improves the cycle efficiency.

For enriched diesel engine, for intake temperature of 30° C ignition delay is found to be 0.76 ms. while in the case of intake temperature of 40° C ignition delay is 0.7 ms. with shorter ignition delay, premixed combustion stage decreases due to which efficiency engine will increase.

The position of injector and injection angle plays a major role in mixture formation and effective flow of air-fuel mixture into the combustion chamber. CFD analysis using FLUENT 6.3.26 was done so as to find the optimum location of the injector. In this present study, two injector positions were taken into consideration. Injector angle was varied as 30°, 45° and 60° and whilst valve position was also varied as 4, 6, 8 and 10 mm for each injector position. The injector angle of 60°, 120 mm from cylinder head and valve lift of 4mm was found to be optimum location of injector position. Based on best performance and safety issue such as backfire problem.

I. INTRODUCTION

The world's resources of oil are limited and non-renewable. Therefore production must reach a peak and then turn down. About half of our oil reserves have been already consumed the half that was easiest to produce. The oil field discovery rate has been declining for 40 years despite extensive exploration with advanced technology, and there is uncertainty about the timing of the peak of oil production. There is no doubt about the fact that oil production will not meet demand in the near future. When that happens oil prices will rise substantially and the global economy will be adversely affected.

The basic solution to these problems will be to use energy resources more efficiently and to switch from fossil fuels to some renewable energy resources. Nuclear, solar, wind and water energy are some of the alternative energy sources. Despite of the nuclear energy all other energy resources are

renewable and environmentally friendly to be used in power generation and power plants.

1.1 ALTERNATE ENGINE FUELS

The accelerated depletion of the fossil fuel reserves and growing vehicular exhaust emission problem has focused the attention on the finding of alternate clean burning fuels for use in internal combustion engines. Broadly three kinds of alternate fuels have been proposed. These are alcohols, biomass based fuels like biogas and producer gas and hydrogen.

From many economical, technical and ecological considerations hydrogen seems to be the most suitable candidate fuel substitute for petroleum fuels. Hydrogen can be obtained from fossil fuels, biomass or by decomposing water either by thermally or by electrolysis. The feasibility of its production from water which is abundant makes is a truly renewable fuel.

Tasteless, odorless and non-toxic by itself, hydrogen produces just clean energy and water vapors upon combustion with air. Thus restoring quantitatively to the environment, the water from which it is produced. Moreover, combustion of hydrogen with air does not give carbon containing pollutants; hence in case it used as an automotive engine fuel, exhaust emissions of smoke, hydrocarbons, carbon monoxide and carbon dioxide are likely to be eliminated.

1.2 HYDROGEN AS AN ALTERNATIVE FUEL FOR IC ENGINES

Future demands for the power units of high thermal efficiency with low pollution emission levels have stimulated endeavors to develop hydrogen fuelled reciprocating internal combustion engines. In the previous studies in this direction, most efforts have been offered to the spark ignition type of engines. It has been widely accepted that an unthrottled lean burn operation may be retainable thereby enhancing thermal efficiency and reducing the oxides of nitrogen in the exhaust. The spark ignition engine however may only be served as a compact power unit, and is not feasible for requirements of larger output power more applicable to heavier traction of some vehicles, ships, and other stationary power supply; which are normally worked by diesel engines.

It is, therefore strongly demanded to establish a hydrogen fuelled compression ignition engine, or simply a hydrogen diesel engine. However, such an attempt has scarcely been reported. If it were attainable, there exists anticipated advantages distinct from SI engine other than the augmented engine scale; the use of higher compression will increase thermal efficiencies on the one hand, and the adoption of direct fuel injection into the combustion space will eliminate the loss in the suction air on the other hand.

The initiative for using hydrogen fuel in CI engine came much recently. Despite the facts that hydrogen, as energy carrier posses attractive energy and ecological characteristics, whereas the reserves of raw materials for hydrogen production are practically unlimited and relatively high cost of hydrogen and complexity of its storage systems hamper its uses as a motor fuel.

Hydrogen can be used in various systems as follows:

- In neat mode in a spark ignition (SI) engine system
- In dual-fuel mode in SI and compression ignition (CI) engine systems
- In fuel cells
- In hybrid electric vehicle systems.

The use of hydrogen in a CI engine is very attractive since CI engines are preferred power plants used in all commercial vehicles.

1.3 HYDROGEN IN CI ENGINE

The concept of using hydrogen as an alternative to diesel fuel in CI engines is recent. As the self-ignition temperature of hydrogen is much higher than that of diesel fuel, hydrogen cannot be ignited by compression. Hence, it requires the use of an external ignition source such as a spark plug or a glow plug. One of the alternative methods is to diesel fuel as a pilot fuel for ignition or by using ignition improvers such as diethyl ether (DEE).

Adapting the fuel delivery system can be effective in reducing or eliminating pre-ignition. Hydrogen fuel delivery system can be classify into three main types

- Hydrogen enrichment.
- Hydrogen port/manifold injection.
- Hydrogen In-cylinder injection.

1.4 HYDROGEN ENRICHMENT

Hydrogen enrichment is the technique in which the air is enriched by using a venture/gas carburetor in the intake manifold. Pilot quantity of diesel is used as an ignition source. The benefit of hydrogen enrichment is that the brake thermal efficiency increases, but the power output of the engine drops down due to the partial replacement of air by gaseous hydrogen, pre-ignition and backfire problems are severe in manifold induction system.

1.5 HYDROGEN PORT/MANIFOLD INJECTION

Hydrogen can be injected in the intake port/manifold by using mechanically or electronically operated injector. Electronic injectors are robust in design with a greater control over the injection timing and injection duration with quicker response to operate under high speed conditions. The position of the injector system on the manifold will determine the whether it is port injection system or manifold injection system. For both the injection systems, the ignition source be diesel. The advantage of hydrogen injection over carbureted system is that with proper injection timing. The backfire and pre-ignition problems can be eliminated.

1.6 DUAL FUEL ENGINE

The dual fuel engine is conventional diesel engine of compression ignition type in which some of the energy released by the combustion of gaseous fuel, while the remaining energy is released from diesel liquid fuel continuously provided throughout, through timed cylinder injection. The dual fuel engine is an ideal multi-fuel engine that operates effectively on a wide range of different fuels while maintain the capacity for operation as a conventional diesel engine.

2. A NUMERICAL MODEL TO PREDICT THE PERFORMANCE OF A CI ENGINE ENRICHED BY HYDROGEN FUEL

2.1 INTRODUCTION

The combustion process in a CI engine is more complex than in SI engine. In a typical compression ignition engine air alone is compressed and so raised to a high temperature during the compression stroke. So the rapid spontaneous ignition of the fuel is possible after it has been injected into the combustion chamber.

Because of heterogeneities of the combustion process in a CI engine. In-cylinder studies of the combustion process have been very difficult. The basic understanding of the processes has been mainly achieved by the researchers from the combustion process and the analysis of cylinder process diagrams. Based on these limited study a few models have been developed to compute the pressure-crank angle changes in the cylinder and performance of the engine.

In typical diesel fuelled CI engine, diesel is injected, towards the end of the compression stroke, so that the fuel is distributed in jet, or in several jets, throughout all or part of the combustion chamber. Distribution of the fuel, mixing with air, evaporation and diffusion to produce a gaseous mixture and chemical reactions to burn the fuel, all have to be accomplished in an extremely short period of time if the engine is to be efficient. There is little time for mixing and evaporation, and the different process referred to above tend to develop.

From the commencement of the injection, the combustion process, as deduced from a study of the cylinder pressure diagrams, may be divided into several stages Figure 2.1.

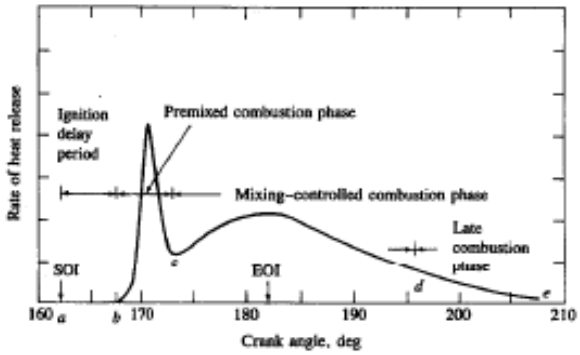

Fig 2.1 Heat release rate diagram identifying different diesel combustion Phases.

In the case of dual fuel operation with diesel as fuel pilot fuel, the method in which hydrogen is introduced to the combustion chamber dictates a lot of its theoretical analysis. However, under the assumption that hydrogen well mixed with air is introduced through intake manifold in a conventional diesel run CI engine makes the combustion analysis a little easy and simple. But. Still there are some problems due to distinct combustion properties of hydrogen that poses few limitations over the theoretical analysis. Nevertheless, with some more simple assumptions fair results could be expected.

2.2 CI ENGINE SIMULATION

Engine simulation refers to the simulation of different processes involved in engine operation and these processes occur cyclically shown in Figure 2.2.

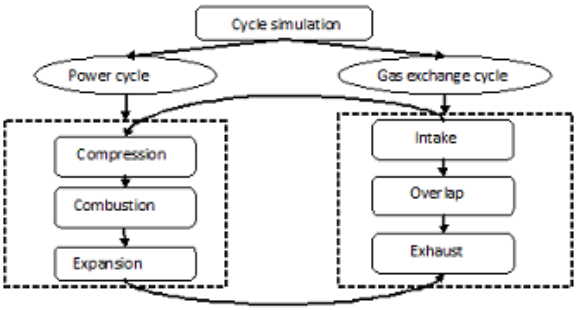

Fig 2.2 sequence of processes followed by cycle-related engine simulations

Figure 2.3 shows a pressure vs. volume plot for a CI engine. In the figure point 1 indicates the closing of inlet valve which is considered as the beginning of compression. Point 2 indicates the end of compression and the beginning of combustion. Point 3 represents the end of combustion and beginning of expansion. Point 4 is the end of expansion and at this point the exhaust valve opens.
Let,

P_a = Ambient pressure

P_1 and V_1 are the pressure and volume before compression.

T_a = Ambient air temperature

T_m =Intake manifold temperature

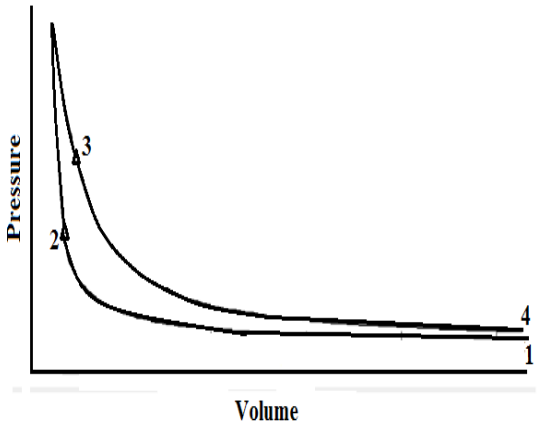

Fig 2.3 Pressure volume diagram of a CI engine

There will be no pressure, temperature drop in the intake manifold as the fuel injected into the intake manifold, cylinder in the case of dual fuel mode. Therefore, T_m=T_a.

2.3 ENGINE KINEMATICS USED IN SIMULATION

The basic geometry of a reciprocating piston engine is shown in following Figure 2.4. The displacement volume V_{dis} is swept out as the piston moves from BDC to TDC.

$$V_{dis} = V_{TDC} - V_{BDC} = \frac{\pi}{4} B^2 S \quad \ldots\ldots (2.1)$$

Since compression ratio,

$$r = \frac{V_{BDC}}{V_{TDC}} \quad \ldots\ldots (2.2)$$

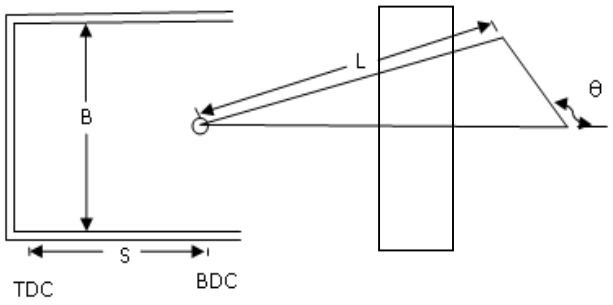

Fig 2.4 Kinematics of engine

And the volume at bottom dead centre and top dead centre can be calculated

$$V_{BDC} = \left[\frac{r}{r-1}\right] \times V_{dis} \ldots\ldots (2.3)$$

$$V_{TDC} = \left[\frac{1}{r-1}\right] \times V_{dis} \ldots\ldots (2.4)$$

With θ denoting the angular displacement of the crank from BDC, and the volume V (θ) at any crank angle is represented by [10, 13],

$$V(\theta) = V_{dis} \times \left[\frac{r}{r-1} - \frac{1-\cos\theta}{2} + \frac{L}{S} - \frac{1}{2}\sqrt{\left(\frac{2L}{S}\right)^2 - \sin^2\theta}\right] \quad \ldots. (2.5)$$

And, Rate of change in volume with respect to every crank angle duration

$$V'(\theta) = \frac{dV}{d\theta} = \frac{V_{dis}}{2} \times \left[\frac{1}{2}\frac{\sin 2\theta}{\sqrt{\left(\frac{2L}{S}\right)^2 - \sin^2\theta}} - \sin\theta\right] \ldots. (2.6)$$

Crank angle is considered to be varying from -180°, at the beginning of compression stroke to 180°, at the end of expansion stroke.

3. CFD ANALYSIS OF MANIFOLD INJECTION

3.1 INTRODUCTION

Computational Fluid Dynamics (CFD) has been most commonly used tool for flow based physical simulation, process evaluation, and component design. CFD, when implemented properly, is a low-cost, rapid, non intrusive, parametric test method. As a design tool, it permits developments with greater reliability and repeatability, at a fraction of the cost and time.

In this chapter, governing equations of motion for compressible reactive flow, heat transfer, etc used by the FLUENT main program were

introduced. Conservation laws of mass, momentum, energy, amount of substance, etc, are governing the fluid flows. It is more common practice in numerical fluid mechanics calculations to compute time or ensemble averaged values of the variable to be calculated.

3.2 MODELING OF INTAKE MANIFOLD INJECTION SYSTEM

Study on the intake manifold for the optimum location consists of three basic steps

1. Numerical Domain Setup
2. Modeling and Computation
3. Evaluation of the Results

These steps are described in the following sections.

3.2.1 Numerical Domain Setup

As part of the pre-processing, one must define a geometry to which the CFD will be applied. This model setup includes the generation of the mesh to define the individual volumes that make up the computational domain. In addition to the creation of the mesh, boundary conditions such as a pressure, velocity, etc., need to be carefully considered in order to accurately reproduce real situations.

3.2.1.1 Geometry

A schematic of the intake manifold system proposed was presented in Figure 3.1. As per the dimensions of the engine and the valve, model was created in ICEM CFD version 12.1 The engine specifications are mentioned in appendix A. Several modeling tools such as fillet, subtracting the area, etc., were used for creating the geometry. The cross section manifold is considered as tapered shape, ratio $(\frac{D_1}{D_2})$ varies depends on engine specifications and it is 0.5-0.9 [14].

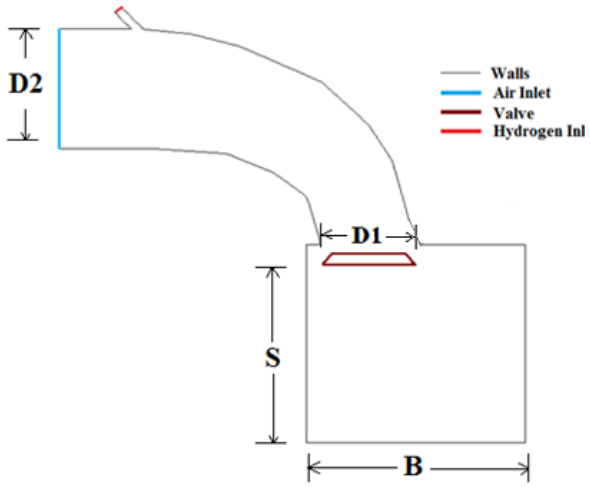

Fig 3.1 Schematic of intake manifold system

Models with different valve lifts, Injector angles and Injector positions were created according to the Table 3.1. Figure 3.2 represents number of the cases which has to be studied for optimum location and angle.

Valve lift	Injector angle	Injector position with reference to cylinder axis
(mm)	(°)	(mm)
4 ,6,8,10	30, 45, 60, 90	70, 120

Table 3.1 Variables of the various components

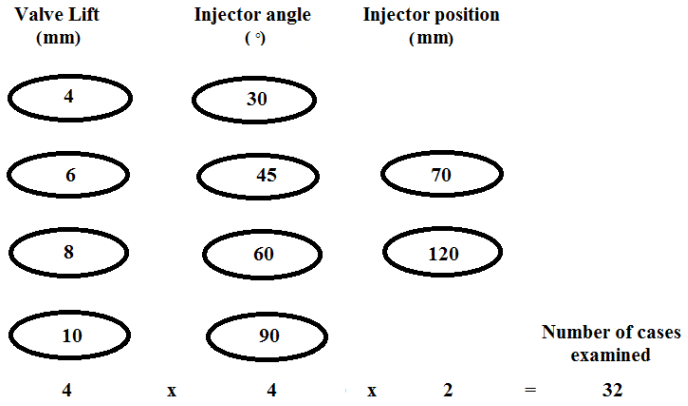

Fig 3.2 Number of cases examined

3.2.1.2 Mesh Generation

To discretise the Navier Stokes equations, the domain must be covered by a computational mesh. The numerical domain and mesh were initially created using ICEM CFD version 12.1 geometry and mesh generation software that is a companion program to the FLUENT version 6.3.26 software. ICEM can be used to create the domain using modeling based geometry tools or to import geometry created in standard CAD programs. Following creation of the geometry, the model is then meshed using a variety of different tools depending upon the problem at hand. Following creation of the geometry and mesh, the boundaries are defined and the model can then exported to a *.uns file for later import directly into FLUENT.

Course, normal and fine meshes were considered. Number of elements for each mesh type was given in Table 3.2.

Cases	Type	Number of Elements
Case 1	Course	90, 343
Case 2	Normal	1, 95, 719
Case 3	Fine	2, 50, 864

Table 3.2 Total Number of Elements for Different Mesh Type

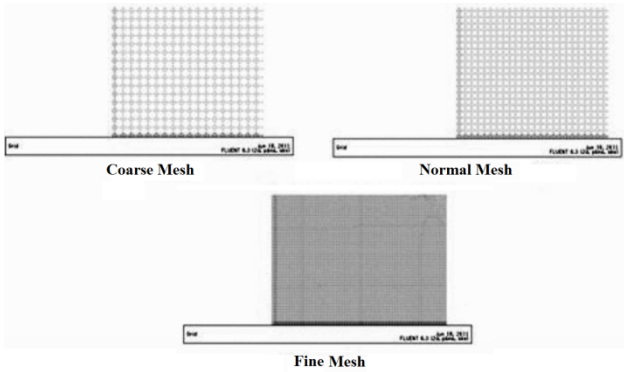

Fig 3.3 Comparison between different type of meshes

3.2.1.3 Governing Equations

There are three groups of basic equations, which are derived from three basic physics laws of conservation. The mass conservation, momentum conservation and energy conservation results in the continuity equation, Navier-stokes equation and energy equation respectively.

Continuity equation

$$\frac{\partial(\rho v_x)}{\partial x}+\frac{\partial(\rho v_y)}{\partial y}=0 \quad \ldots\ldots\ldots\ldots(3.1)$$

Momentum equation

In x-direction,

$$\frac{\partial(\rho v_x v_x)}{\partial x}+\frac{\partial(\rho v_x v_y)}{\partial y}=\rho g_x+\frac{\partial}{\partial x}\left(\mu_e\frac{\partial v_x}{\partial x}\right)+\frac{\partial}{\partial y}\left(\mu_e\frac{\partial v_x}{\partial y}\right)+\tau_x \quad \ldots\ldots\ldots\ldots (3.2)$$

In y-direction,

$$\frac{\partial(\rho v_x v_y)}{\partial x}+\frac{\partial(\rho v_y v_y)}{\partial y}=\rho g_y+\frac{\partial}{\partial x}\left(\mu_e\frac{\partial v_y}{\partial x}\right)+\frac{\partial}{\partial y}\left(\mu_e\frac{\partial v_y}{\partial y}\right)+\tau_y \quad \ldots\ldots\ldots\ldots\ldots\ldots(3.3)$$

Energy equation

$$\frac{\partial}{\partial x}(\rho v_x C_p T_o)+\frac{\partial}{\partial y}(\rho v_y C_p T_o)=\frac{\partial}{\partial x}\left(K\frac{\partial T_o}{\partial x}\right)+\frac{\partial}{\partial y}\left(K\frac{\partial T_o}{\partial y}\right)+W^V+E_K+Q_V+\emptyset \quad \ldots\ldots\ldots\ldots (3.4)$$

3.2.1.4 Turbulence Modeling

Fluid flow with a very high Reynolds number and high Rayleigh's number is called turbulent flow. Since the fluid flow inside the conditioned space is turbulent, a turbulent model must be considered for calculating the fluid properties in Fluent. In turbulent flow, velocity fields fluctuate. These fluctuations mix with transport quantities such as momentum, energy and species concentration, consequently the transport quantities fluctuate as well.

The exact governing equation, however, can be time-averaged or ensemble-averaged or otherwise manipulated to remove the small scales. As a result a modified set of equations are created from this operation. Unknown variables are generated in the modified equations, and these variables are determined as known quantities by using the turbulence model.

3.2.1.5 Transport Equations for the RNG k-ε Model

The standard k-ε model is a semi-empirical model, based on model transport equations for the turbulence kinetic energy (k) and its dissipation rate (ε). The model transport equation for k is derived from the exact equation, while the model transport equation for ϵ was obtained using physical reasoning and bears little resemblance to its mathematically exact counterpart.

In the derivation of the k-ε model, it was assumed that the flow is fully turbulent, and the effects of molecular viscosity are negligible. The standard k-ε model is therefore valid only for fully turbulent flows.

The turbulent kinetic energy k and its rate of dissipation ϵ are obtained from the following transport equations:

$$\frac{\partial}{\partial x_j}(\rho k u_i)=\frac{\partial}{\partial x_j}\left[\left(\mu+\frac{\mu_t}{\sigma_k}\right)\frac{\partial k}{\partial x_j}\right]+G_k+G_b-\rho\epsilon-Y_M+S_k \quad \ldots\ldots\ldots\ldots (3.5)$$

$$\frac{\partial}{\partial x_j}(\rho\epsilon u_i)=\frac{\partial}{\partial x_j}\left[\left(\mu+\frac{\mu_t}{\sigma_\epsilon}\right)\frac{\partial\epsilon}{\partial x_j}\right]+C_{1\epsilon}\frac{\epsilon}{k}(G_k+C_{3\epsilon}G_b)-C_{2\epsilon}\rho\frac{\epsilon^2}{k}+S_\epsilon \quad \ldots\ldots (3.6)$$

Model constants

The model constants $C_{1\epsilon}$, $C_{2\epsilon}$, C_μ, σ_k and σ_ϵ have the following default values.

$C_{1\epsilon}=1.44$, $C_{2\epsilon}=1.92$, $C_\mu=0.09$, $\sigma_k=1.0$, $\sigma_\epsilon=1.3$.

Modeling the Turbulent Viscosity

The turbulent viscosity μ_t is computed by combining k and ϵ as follows:

$$\mu_t = \rho C_\mu \frac{k^2}{\epsilon} \quad \ldots\ldots\ldots\ldots \quad (3.7)$$

3.2.1.6 Boundary conditions

To define a problem that results in a unique solution it is necessary to specify the information on the flow variables at the domain boundaries. It is important to define these correctly as they can have a significant impact on the numerical solution. Boundary conditions used to define the problem were given in Figure 3.4

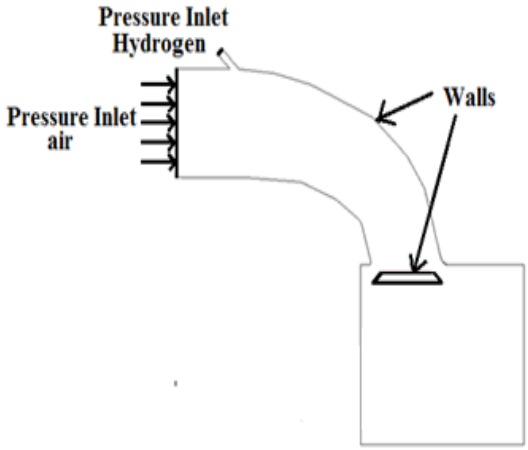

Fig 3.4 Boundary conditions

The pressure inlet of air was taken at atmospheric pressure; hydrogen was injected inside the intake manifold with a pressure of 2 bar. Usually it varies from 1- 3 bar, it depends upon the manifold pressure before hydrogen is injected. The position of inlet valve changes with respect to piston movement during period of suction stroke, the maximum valve lift was considered as 10 mm.

3.2.2 Mixture

Understanding this flow phenomena helps to design the right combustion chamber for specific application such as in direct injection engine, the injected fuel is directed to spark plug, and creation of swirl or tumble is important for better mixture formation. Adaption of grid was done and the mixture characteristics were studied using Fluent 6.3.26.

Fluid material input is required and the following has been used

Table 3.3 Material properties

Material	Density (kg/m^3)	Dynamic viscosity ($kg\ m^{-1}s^{-1}$)	Specific heat c_p (kJ/kg K)
Air	1.225	1.7894×10^{-5}	1.006
Hydrogen	0.081	8.41×10^{-6}	14.28

3.2.3 Solver Controls

FLUENT offers a wide variety of solvers, discretisation schemes and variables this can affect the solution quality and convergence. A summary of the key solution parameters chosen are discussed below, however much more detail may be found in the Fluent User Guid.

In Fluent, the process to obtain the computational solution involves of two stages.

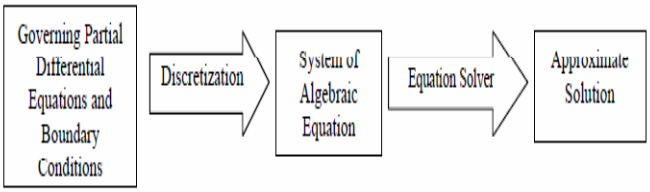

Fig 3.5 Methodology of fluent

Once the approximate solution was found, iterations will start so as to converge the solution. Table 3.4 gives the convergence criteria given to FLUENT software. The solution will be converged when the tolerance between the old and new value of the parameter is less than the convergence criteria mentioned in the Table 3.4

	Maximum Number of Initial Iterations	Correction Tolerance	Residual Tolerance	Relaxation Factor
Pressure	10	0.25	0.0001	1
Momentum	5	0.05	0.0001	1
Energy	5	0.05	0.0001	1

Table 3.4 Convergence criteria

Once the convergence criteria are satisfied, the solution for the problem is ready.

4. RESULTS AND DISCUSSION

This chapter includes the comparison of theoretical results of hydrogen enriched diesel fuel with pure diesel. Further, the results obtained from CFD analysis on intake manifold injection are discussed.

4.1 THERMODYNAMIC ANALYSIS OF CI ENGINE ENRICHED BY HYDROGEN FUEL

When a small amount of hydrogen is added to the intake air, the combustion process of the internal combustion engines could be considerably enhanced.

The thermodynamic analysis performed under the following two conditions.

(i) Case I: engine runs on diesel only.

(ii) Case II: engine runs on diesel as primary fuel and hydrogen as secondary fuel.

Table 4.1 Mass of fuels

Case no.	Mass of diesel (kg/min)	Mass of hydrogen (kg/min)
I	0.6	-
II	0.5	0.1

4.1.1 Comparison of Theoretical Results of Case I and Case II

4.1.1.1 Cylinder Pressure and Volume

Figure 4.1 illustrates that, with the addition of hydrogen fuel to the diesel, the pressure rises suddenly with in small crank angle duration compared to the pure diesel. And this is because combustion process improvement by the means of combustion reduction because of superior combustion and flame propagation properties of hydrogen.

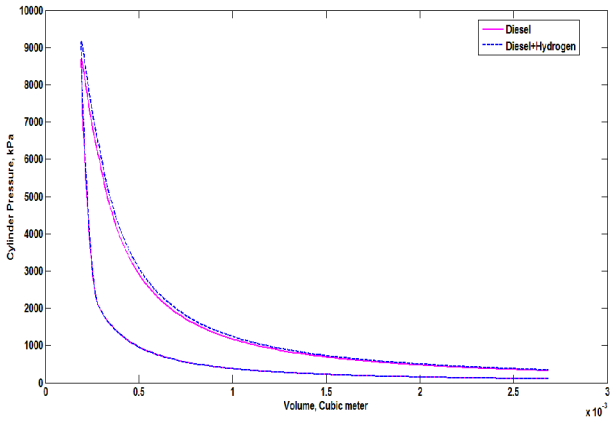

Fig 4.1 Cylinder pressure-volume

4.1.1.2 Cylinder Pressure

Figure 4.2 and Figure 4.3 shows the variation in the pressure-CA diagram for diesel fuel and for a hydrogen operated dual fuel engine. The peak pressure of hydrogen operated engine is found to be 91.7 bar, compared with 87.1 bar for the diesel operated engine at 1500 rpm.

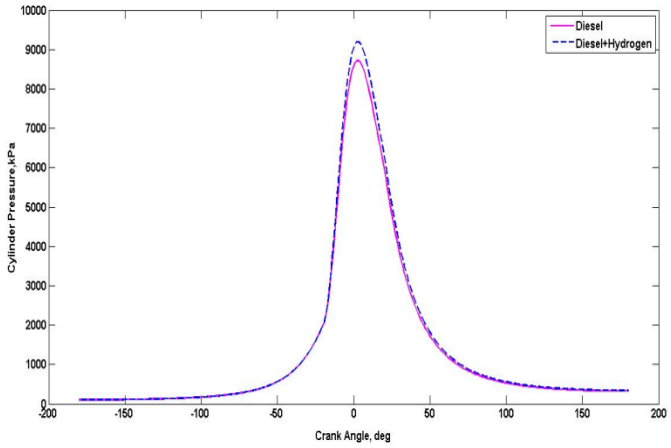

Fig 4.2 Cylinder Pressure Data

There is a shift in peak pressure value towards top dead centre (TDC) by 5^{o} for a hydrogen operated engine compared with diesel engine. The shift in peak pressure towards TDC may increases the overall efficiency of the engine. There is a sharp rise in the pressure for hydrogen operated engine compared with a diesel engine; this is due to the instantaneous combustion of hydrogen.

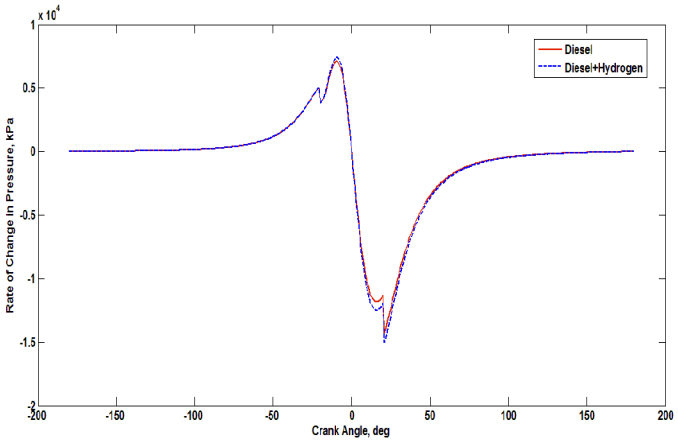

Fig 4.3 Cylinder Pressure Rate

4.1.1.3 Cylinder temperature

Figure 4.4 illustrates that temperature rise with addition of hydrogen fuel. With the addition of hydrogen fuel to diesel the rise in temperature observed. Because of hydrogen has high calorific value when compared to diesel fuel and high flammability limits.

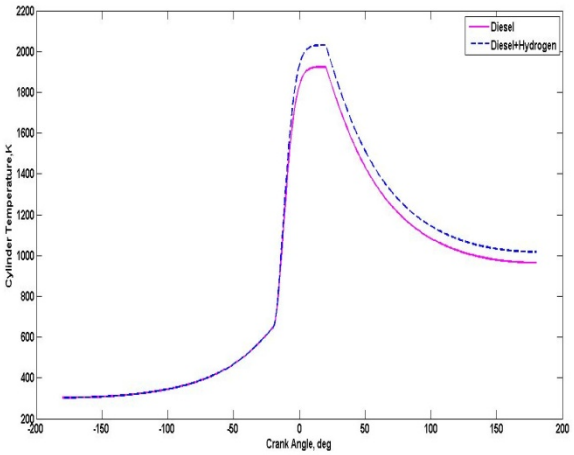

Fig 4.4 Cylinder Temperature

4.1.1.4 Heat release rate

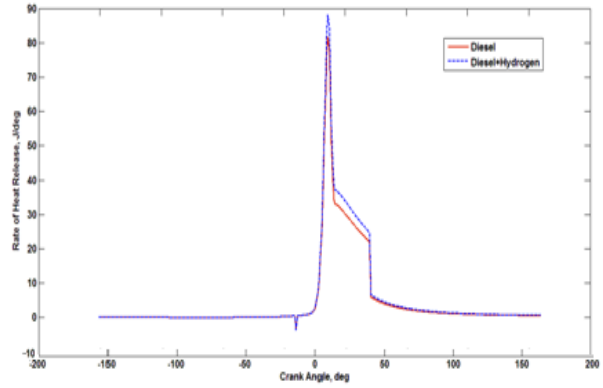

Fig 4.5 Net Heat Release Rate

The combustion duration reduction is due to reduced mixing controlled combustion phase invoking higher net heat release rate. The reduction of mixing controlled combustion phase is due to the flame propagation of homogenous hydrogen-air mixture through the combustion chamber. The flame propagation improves the diffusion process between the hot air and diesel vapours causing its faster completing. The diffusion process improvement causes higher heat utilization and higher net heat release respectively.

Figure 4.5 represents the variation in the rate of heat release with CA at 1500 rpm for a hydrogen operated engine compared with a diesel operated engine. The combustion in these two configurations starts at the same CA of about 20^0 before ignition TDC. As explained earlier for diesel engine operation, there are three phases of combustion, namely the premixed combustion phase and the late combustion phase. The peak heat rate of a hydrogen operated engine is higher 88.2 J/^{o} CA, compared with 86.9 J/^{o} CA for a diesel-fuelled. The maximum heat addition occurs at nearer to the TDC for hydrogen operation, which makes the cycle efficiency, improves.

4.1.2 Effect of Intake Temperature on Ignition Delay of Hydrogen enriched CI engine

4.1.2.1 Cylinder Pressure

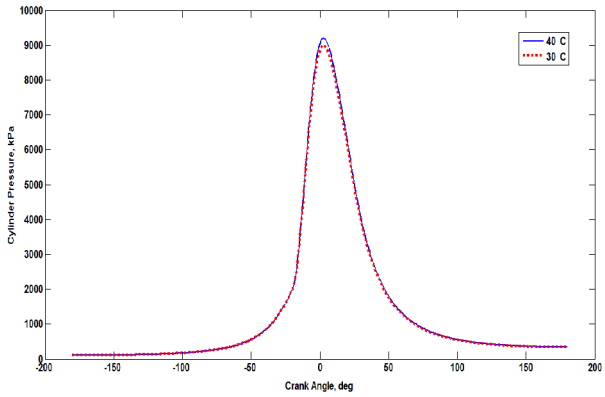

Fig 4.6 Cylinder pressure with the variation of inlet air temperature

An increase in inlet air temperature will affect the cylinder pressure crank angle history. A small decrease of cylinder pressure was observed with an increase in inlet air temperature. However, the peak pressures were observed at the same crank angle.and the peak pressure was found to be 91.9 bar at 40° C inlet air temperature.

4.1.2.2 Cylinder Temperature

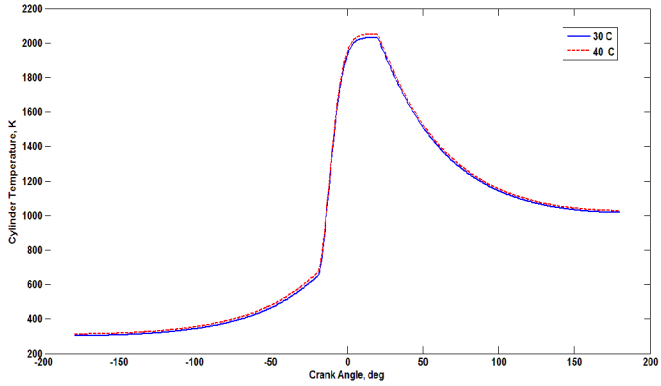

Fig 4.7 Cylinder temperature with the variation of inlet air temperature

Cylinder temperature with the variation of inlet air temperature is also presented in Figure 4.7. Average cylinder temperature increases with an increase in inlet air temperature. And ignition delay period also decreased when the air inlet temperature changes from 30° C to 40° C. Almost an average of 50° K cylinder temperature increased when inlet air temperature changes from 30° C to 60° C. This change in average cylinder temperature will play an

important role on engine out NOX emissions. Table 4.2 shows the variation of ignition delay period with respect to air inlet temperature. The decrease in delay period helps to improving the premixed combustion process.

Table 4.2 Ignition Delay

Intake temperature(°C)	Ignition delay(°CA)	Ignition delay (ms)
30	4.57	0.76
40	4.31	0.70

5.1.2.3 Rate of heat release

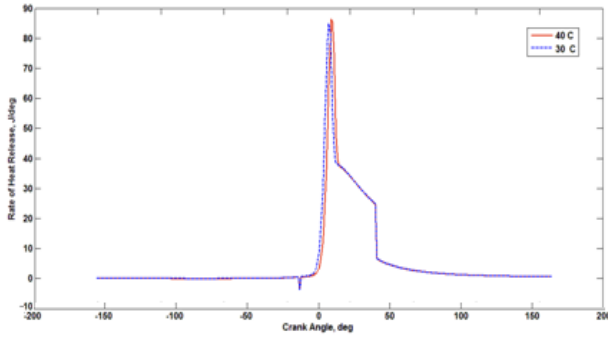

Fig 4.8 Rate of heat release with the variation of inlet air temperature

Figure 4.8 shows rate of heat release analysis for diesel and hydrogen fuel mixture when inlet air temperature changes from 30° C to 40° C. The start of combustion is indicated by the crank angle degree when the rate of heat release curve moves from negative to positive value. On the other hand, the higher the inlet air temperature, the lower the premixed and diffusion burning peaks. It is also true that the premixed combustion stage decreases with shorter ignition delay. And maximum heat release was found to be 86.42 J/deg at 40°C inlet air temperature compared to 30° C inlet air temperature.

4.2 RESULTS OBTAINED FROM CFD ANALYSIS

The position of injector and injection angle plays a major role in mixture formation and effective flow of air-fuel mixture into the combustion chamber. In this present study, two injector positions were taken into consideration. Injector angle was varied as 30°, 45° and 60° and whilst valve position was also varied as 4, 6, 8 and 10 mm for each injector position. As hydrogen diffuses quickly into air, the formation of hydrogen-air mixture was not that tough. But a proper formation of hydrogen-air mixture before entering into the combustion chamber is required for better performance.

4.2.1 Velocity contours of 4, 6, 8, 10 mm of valve lift for 30° injector angle placed at 70 mm from cylinder axis

In this section, the results obtained from the CFD analysis of 4, 6, 8, 10 mm of valve lift for 30° injector angle placed at 70 mm from the cylinder axis were shown in Figure 5.9

As shown in Figure 5.9, hydrogen flows into the combustion chamber along the wall of the inlet manifold. The concentration of hydrogen was found to be unevenly distributed in the combustion chamber at 4 and 6 mm valve lift compared to the 8 and 10 mm valve lift positions. Hydrogen-air mixture requires very little amount of ignition energy. If the residual gases remain inside the combustion chamber after the completion of one cycle, early injection (8 and 10 mm valve lift) of hydrogen may lead to self ignition. Due to which backfire / flashback may occur and may damage walls of the cylinder. Swirling action inside the combustion chamber was lacking.

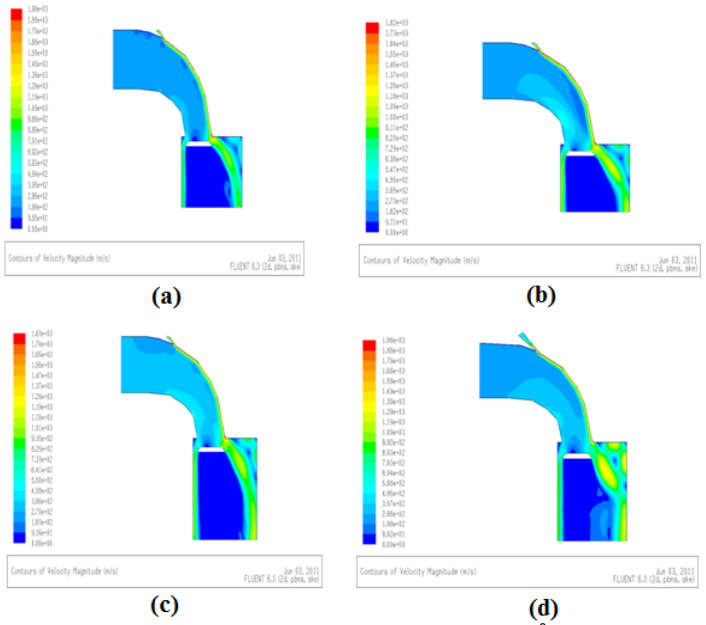

Fig 4.9 Contours of velocity magnitudes at 30° injector angle, 70mm from cylinder axis at (a) 4, (b) 6, (c) 8 and (d) 10 mm valve lift

4.2.2 Velocity contours of 4, 6, 8, 10 mm of valve lift for 45° injector angle placed at 70 mm from cylinder axis

As shown in Figure 4.10, hydrogen flows into the combustion chamber along the wall of the inlet manifold. The concentration of hydrogen was found to be unevenly distributed in the combustion chamber at 4 and 6 mm valve lift compared to the 8 and 10 mm valve lift positions. Hydrogen-air mixture

requires very little amount of ignition energy. As the residual gases remain inside the combustion chamber after the completion of one cycle, early injection (8 and 10 mm valve lift) of hydrogen may lead to self ignition. Due to which backfire / flashback may occur and may damage walls of the cylinder. Compared to 30° injector angle, 45° injector angle gives better swirling action inside the combustion chamber.

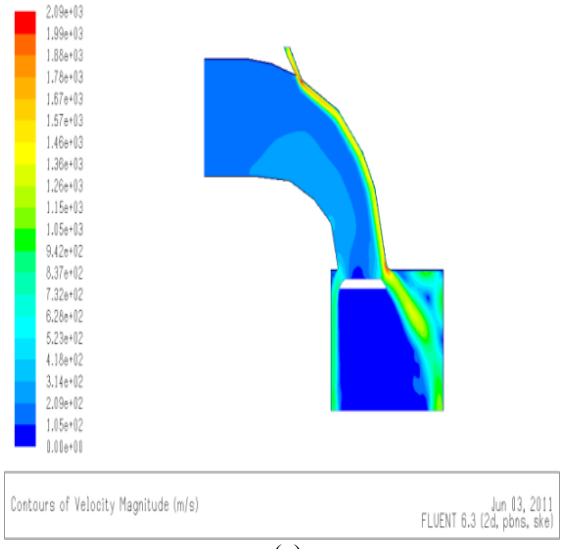

(a)

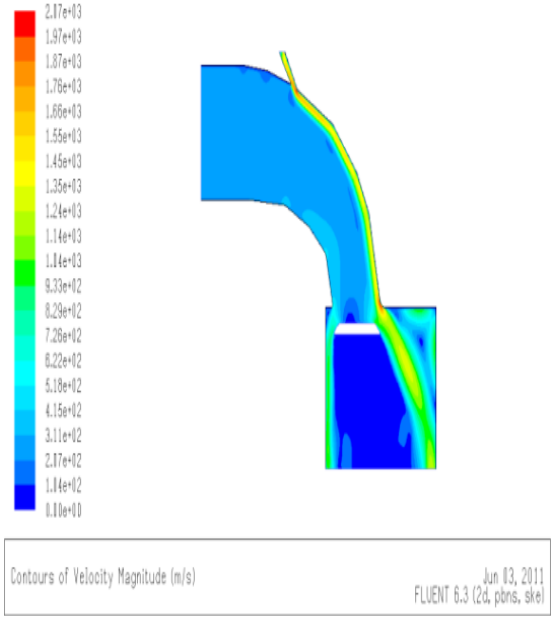

(b)

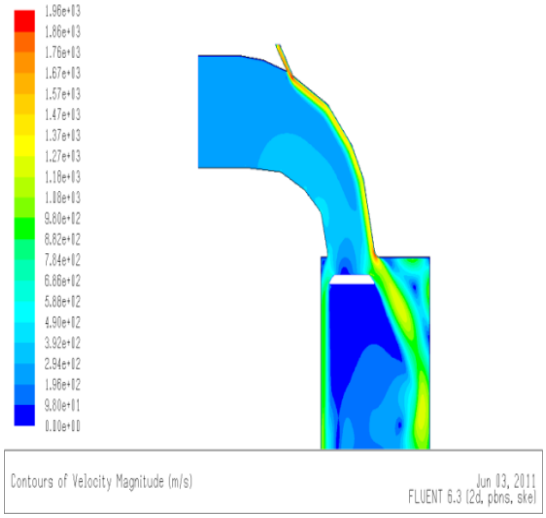

(c)

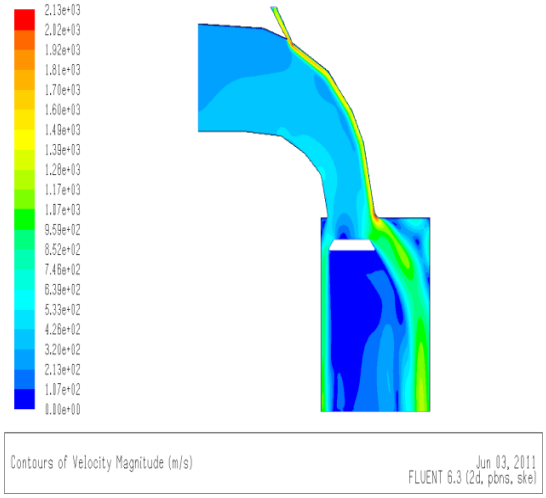

(d)

Fig 4.10 Contours of velocity magnitudes at 45° injector angle, 70mm from cylinder axis at (a) 4, (b) 6, (c) 8 and (d) 10 mm valve lift

4.2.3 Velocity contours of 4, 6, 8, 10 mm of valve lift for 60° injector angle placed at 70 mm from cylinder axis

At 4 and 6 mm valve lift position, the hydrogen enters into inlet manifold axially to injector and enters into the combustion chamber along with the air. This was not the case with 8 and 10 mm valve lift positions. Compared to 30° and 45° injector angles, 60° gives better swirling action inside the combustion chamber.

By comparing the above three cases, 60° angle found to be best for injecting hydrogen.

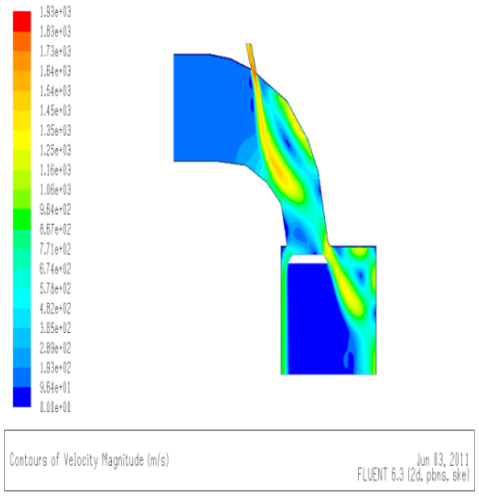

(a)

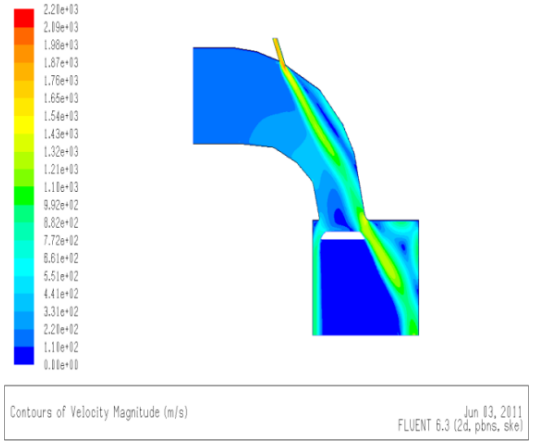

(b)

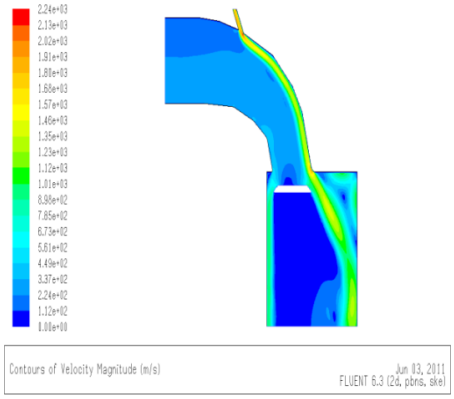

(c)

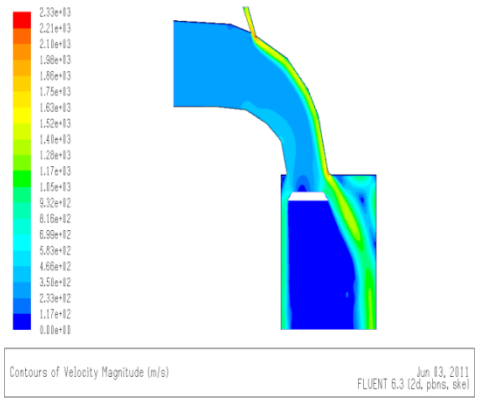

(d)

Fig 4.11 Contours of velocity magnitudes at 60° injector angle, 70mm from cylinder axis at (a) 4, (b) 6, (c) 8 and (d) 10 mm valve lift

4.2.4 Velocity contours of 4, 6, 8, 10 mm of valve lift for 30° injector angle placed at 120 mm from cylinder axis

As shown in Figure 4.12, hydrogen flows into the combustion chamber along the wall of the inlet manifold. The concentration of hydrogen was found to be unevenly distributed in the combustion chamber at 4 and 6 mm valve lift compared to the 8 and 10 mm valve lift positions. Compared to 30° injector angle of 70 mm position, 120 mm position gives the better swirling action inside the combustion chamber.

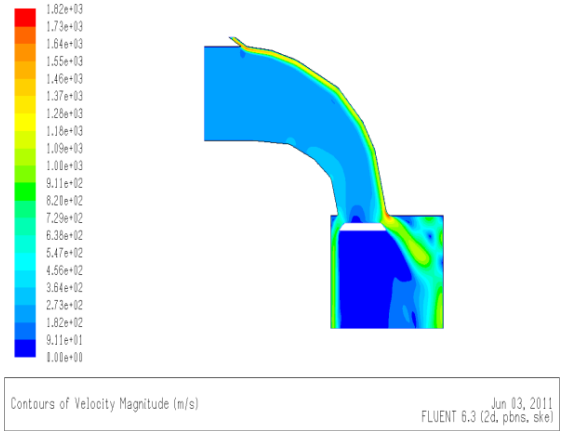

(a)

ISSN 2321-6905
October-2015

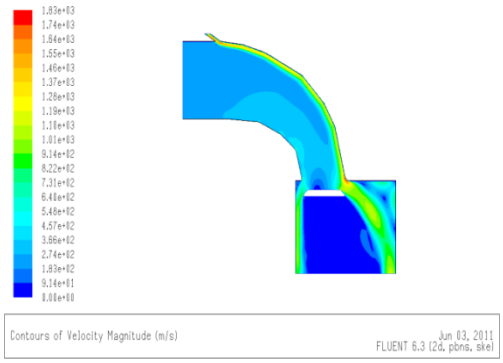

(b)

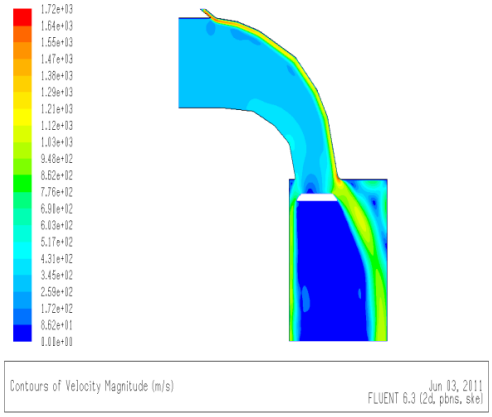

(c)

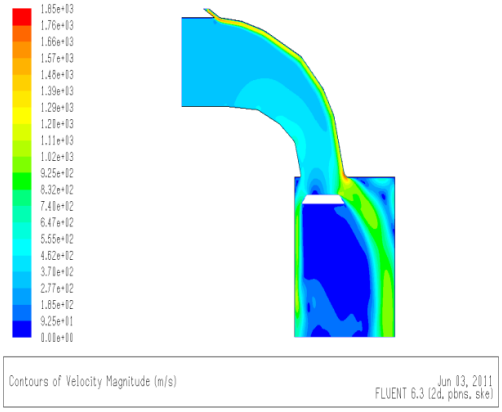

(d)

Fig 4.12 Contours of velocity magnitudes at 30° injector angle, 120 mm from cylinder axis at (a) 4, (b) 6, (c) 8 and (d) 10 mm valve lift

4.2.5 Velocity contours of 4, 6, 8, 10 mm of valve lift for 45° injector angle placed at 120 mm from cylinder axis

For 6 mm position, the hydrogen enters into inlet manifold axially to injector and enters into the combustion chamber along with the air. . This was not the case with 4, 8 and 10 mm valve lift positions.

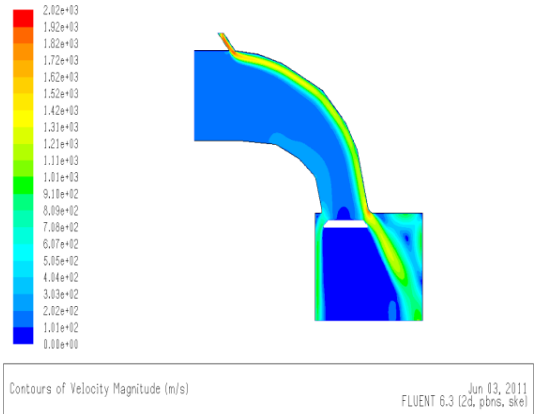

(a)

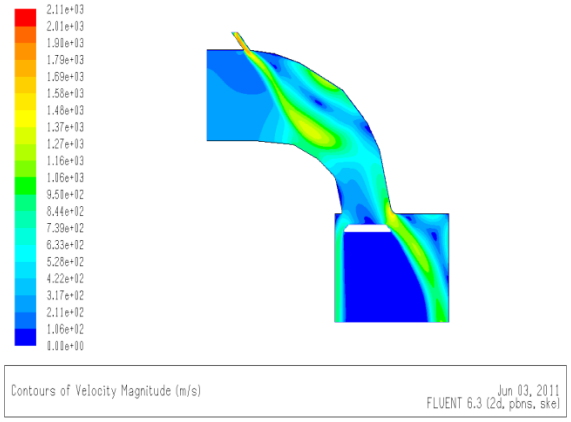

(b)

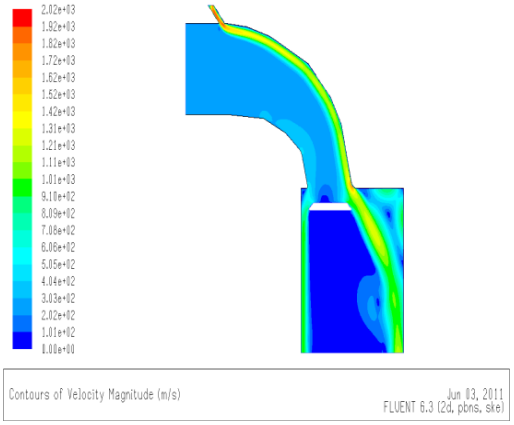

(c)

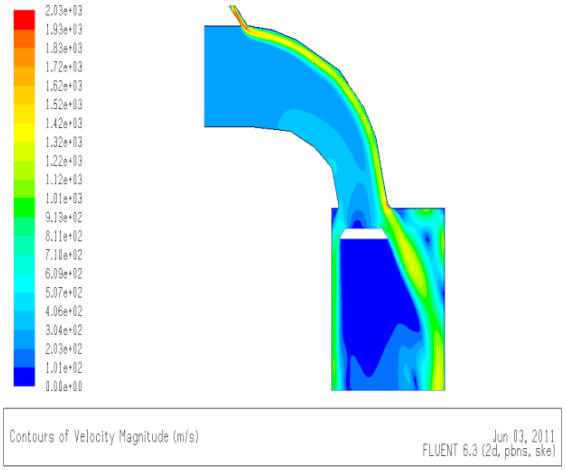

(d)

Fig 4.13 Contours of velocity magnitudes at 45° injector angle, 120 mm from cylinder axis at (a) 4, (b) 6, (c) 8 and (d) 10 mm valve lift

As shown in Figure 4.13, hydrogen flows into the combustion chamber along the wall of the inlet manifold. The concentration of hydrogen was found to be unevenly distributed in the combustion chamber at 4 and 6 mm valve lift compared to the 8 and 10 mm valve lift positions. Hydrogen-air mixture requires very little amount of ignition energy. As the residual gases remain inside the combustion chamber after the completion of one cycle, early injection (8 and 10 mm valve lift) of hydrogen may lead to self ignition. Due to which backfire / flashback may occur. Compared to 30° injector angle, 45° injector angle gives better swirling action inside the combustion chamber.

4.2.6 Velocity contours of 4, 6, 8, 10 mm of valve lift for 60° injector angle placed at 120 mm from cylinder axis

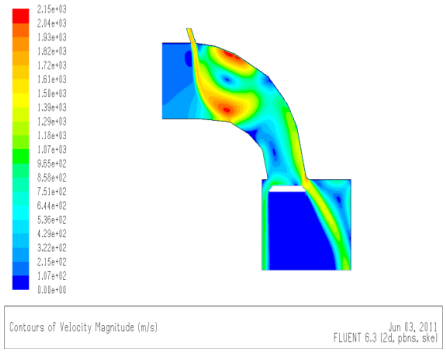

(a)

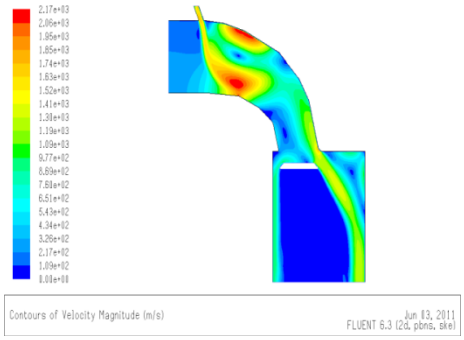

(b)

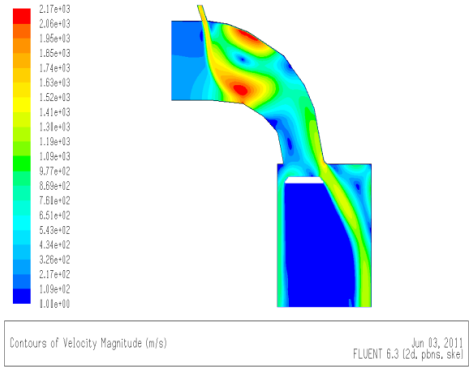

(c)

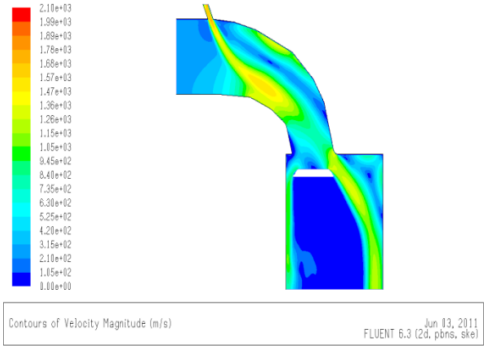

(d)

Fig 4.14 Contours of velocity magnitudes at 60° injector angle, 120 mm from cylinder axis at (a) 4, (b) 6, (c) 8 and (d) 10 mm valve lift

As shown in Figure 4.14, hydrogen flows into the combustion chamber along the wall of the inlet manifold. The concentration of hydrogen was found to be unevenly distributed in the combustion chamber at 4 and 6 mm valve lift compared to the 8 and 10 mm valve lift positions. Hydrogen-air mixture requires very little amount of ignition energy. As the residual gases remain inside the combustion chamber after the completion of one cycle, early injection (8 and 10 mm valve lift) of hydrogen may lead to self ignition. Due to which backfire / flashback may occur

and may damage walls of the cylinder. Compared to 45° injector angle, 60° injector angle gives the better swirling action inside the combustion chamber.

CONCLUSIONS

On the basis of observations and the theoretical analysis obtained during the modeling of the CI engine enriched by hydrogen fuel on a single cylinder compression ignition engine, the following conclusions are drawn from the present study

- The peak cylinder pressure of hydrogen enriched CI engine and diesel operated engine are found to be 91.7 bar and 87.1 bar at 1500 rpm respectively.
- The cylinder temperature of hydrogen enriched CI engine is found to be 1997 K and for diesel operated engine, it was found to be 1898 K at 1500 rpm.
- The rate of heat release of hydrogen enriched CI engine is found to be 88.2 J/deg, compared with 86.9 J/deg for the diesel engine at 1500 rpm. The maximum heat release occurs at nearer to the TDC for hydrogen operation, which makes the cycle efficiency, improves.
- For enriched diesel engine, 0.76 ms ignition delay was found for intake temperature of 30°C. While in case of intake temperature of 40°C, ignition delay was found to be 0.7 ms. With shorter ignition delay, premixed combustion stage decreases due to which efficiency engine will increase.
- The injector angle of 60°, 120 mm from cylinder head and valve lift of 4mm was found to be optimum location of injector position, based on safety issue.

REFERENCES

1. Abdel-Aala, H.K., Sadika, M., Bassyounia, M., Shalabib, M. "A new approach to utilize Hydrogen as a safe fuel". International Journal of Hydrogen Energy 30 (2005), pp. 1511 – 1514.

2. Andras Horvath., Zoltan Horvath. "Application of CFD Numerical Simulation for Intake Port Shape Design of a Diesel Engine". Journal of Computational and Applied Mechanics, Vol. 4, No. 2, (2003), pp. 129-146.

3. Ali Hocine., Bernard Desmet., Smaïl Guenoun. "Numerical study of the influence of diesel post injection and exhaust gas expansion on the thermal cycle of an automobile engine". Applied thermal Engineering 30 (2010) 1889-1895.

4. Ali Sanli. , Ahmet, N. Ozsezen., Ibrahim Kilicaslan., Mustafa Canakci. "The influence of engine speed and load on the heat transfer between gases and in-cylinder walls at fired and motored conditions of an IDI diesel engine". Applied Thermal Engineering 28 (2008) 1395-1404.

5. Chow, A., Wyszynski, M.L. **"**Thermodynamic Modelling Of Complete Engine Systems a Review**".** Proceedings of the Institution of Mechanical Engineers, Part D: Journal of Automobile Engineering 1999 213: 403.

6. Das L.M. "Hydrogen-oxygen reaction mechanism and its implication to hydrogen engine combustion". Int. J. Hydrogen Energy 1996, vol.21. No.8, pp.703-715.

7. Demuynck, J., De Paepe, M., Huisseune, H., Sierens, R., Vancoillie, J., Verhelst, S." On the applicability of empirical heat transfer models for hydrogen combustion engines". Int.J.Hydrogen Energy., 2011, 36, 975-984.

8. Ding, Yu. Douwe Stapersma. Grimmelius, T Hugo. "Cylinder Process Simulation with Heat Release Analysis in Diesel Engine" .IEEE 2009, 978-1-4244-2487-0/09.